

## Advancing Metal-Air Battery Efficiency: MnO<sub>2</sub> Electrocatalyst Synthesized via Electrochemical Method

Giska Koesumasari Putri

Chemical Engineering, Sepuluh Nopember Institute of Technology, East Java, Indonesia

### Article Info

#### Article history:

Received Mar 24, 2025  
Revised Apr 27, 2025  
Accepted May 25, 2025  
OnlineFirst Jun 22, 2025

#### Keywords:

Electrocatalyst  
Metal Air Battery  
MnO<sub>2</sub>

### ABSTRACT

**Purpose of the study:** This study investigates the effect of electrode quantity and voltage on MnO<sub>2</sub> nanoparticle yield and characteristics under acidic and basic conditions, while also evaluating MnO<sub>2</sub>'s potential as an electrocatalyst in metal-air batteries.

**Methodology:** Synthesis of MnO<sub>2</sub> was carried out by electrolysis of KMnO<sub>4</sub> solution with stirring using a magnetic stirrer. In acidic conditions, H<sub>2</sub>SO<sub>4</sub> was used and the electrolysis process lasted for 30 minutes, while in basic conditions, 0.1 M KOH was used up to pH 9 and electrolysis for 24 hours. The research variables included voltage (2V and 4V) and the number of carbon electrodes (1 pair and 4 pairs). The electrolysis results were separated using a centrifuge, washed with demineralized water, and dried in a furnace.

**Main Findings:** MnO<sub>2</sub> from electrolysis in acidic conditions tends to have a low crystalline structure, while in basic conditions it is amorphous with a larger surface area. The addition of electrodes and voltage reduces the surface area and increases particle agglomeration. Cyclic voltammetry tests show the ability of MnO<sub>2</sub> to reduce O<sub>2</sub> at all variables, in accordance with the standard oxygen reduction potential. Linear polarization tests show that MnO<sub>2</sub> synthesized in acidic conditions has better electrocatalytic activity than that synthesized in basic conditions.

**Novelty/Originality of this study:** This study contributes data on the effect of electrolysis parameters on the yield and characteristics of MnO<sub>2</sub> as an electrocatalyst, and shows the best synthesis conditions for application in metal-air batteries.

This is an open access article under the [CC BY](https://creativecommons.org/licenses/by/4.0/) license



### Corresponding Author:

Giska Koesumasari Putri,  
Chemical Engineering, Sepuluh Nopember Institute of Technology, Jl. Teknik Kimia, Keputih, Kec. Sukolilo, Kota SBY, Jawa Timur 60111, Indonesia.  
Email: [gkputrikoes21@gmail.com](mailto:gkputrikoes21@gmail.com)

## 1. INTRODUCTION

The use of metal-air batteries is currently one of the topics of interest in the development of alternative energy [1], [2]. This battery has a high capacitance because it uses oxygen from the air as a reaction material, not stored in the cell. In addition, the anode metal used is generally abundant in nature, making this battery more economical [3], [4]. The simple and lightweight design increases energy density and efficiency of use [5], [6]. Metal-air batteries are also non-toxic, environmentally friendly, and suitable for electronic, medical, and transportation applications.

However, metal-air battery technology still has several significant technical weaknesses. The efficiency at the anode tends to be low due to corrosion and the formation of a passivation layer that inhibits the reaction [7], [8]. This passivation layer can shorten battery life and reduce system performance. On the other hand, at the

cathode, the oxygen reduction reaction is slow and has low reversibility [9], [10]. Therefore, an effective electrocatalyst material is needed to accelerate the reaction at the cathode [11], [12].

Transition metal oxides are promising candidates for electrocatalyst materials because they are cheap, abundant, and environmentally friendly [13], [14]. One of the materials that has been widely studied is manganese dioxide ( $\text{MnO}_2$ ).  $\text{MnO}_2$  has various crystalline forms such as  $\alpha$ -,  $\beta$ -,  $\gamma$ -, and  $\delta$ - $\text{MnO}_2$ , each of which has a unique tunnel structure [15]. This structure affects electrocatalytic activity because it affects the ability to transfer oxygen. Therefore,  $\text{MnO}_2$  is widely used for selective catalysts, ion exchangers, and other energy applications.  $\text{MnO}_2$  synthesis can be carried out through various methods, such as chemical methods (facile hydrothermal or wet methods) and electrochemical methods [16], [17]. Chemical methods generally require expensive chemicals and relatively long processes [18], [19]. In contrast, electrochemical methods offer advantages in terms of time efficiency and high product purity. The results of synthesis through electrochemistry are greatly influenced by parameters such as solution concentration, voltage, and number of electrodes. Control over these parameters allows for the regulation of particle size and morphology of the final product [20], [21].

The study by Worku et al. [16] explored the recent development of  $\text{MnO}_2$ -based oxygen catalysts for rechargeable zinc-air batteries, focusing on  $\text{MnO}_2$ -based materials in general and how to optimize them through various material strategies. Meanwhile, the study by Zamani-Meymian et al. [22] developed a bifunctional catalyst based on  $\text{CoO}:\text{MnO}_2@\text{C}$  supported by carbon cloth fibers for the air cathode of zinc-air batteries, with a high-quality electrocatalyst design approach. Both previous studies contributed significantly to the understanding of  $\text{MnO}_2$ -based materials and catalyst design, but focused more on the application and optimization of existing materials. The current study offers a new approach by using an electrochemical method to synthesize  $\text{MnO}_2$ , which has not been specifically described in previous studies, to improve the efficiency of metal-air batteries, focusing on the impact of synthesis conditions (number of electrodes, voltage, and acid-base environment) on the yield and characteristics of  $\text{MnO}_2$ . This makes the current research have novel value in the synthesis strategy and exploration of the efficiency of  $\text{MnO}_2$  electrocatalysts.

The crystallinity of the resulting particles also varies depending on the synthesis conditions. XRD shows that  $\text{MnO}_2$  synthesized under acidic conditions tends to be more crystalline, while under basic conditions it tends to be amorphous [23], [24]. This difference is caused by temperature and reaction time which affect the crystal formation process. This crystallinity is closely related to the electrocatalyst performance, where a good crystalline structure supports more optimal oxygen reduction reaction activity [25], [26]. Therefore, it is important to compare the electrocatalytic performance of  $\text{MnO}_2$  produced under different synthesis conditions. Given the low yield in previous studies, further studies are needed by varying electrolysis parameters such as voltage and number of electrodes. The goal is to improve the efficiency of  $\text{MnO}_2$  synthesis in acidic and basic conditions. In addition, further characterization of the morphology and crystal structure is needed to evaluate the potential of  $\text{MnO}_2$  as an electrocatalyst in metal-air batteries [27], [28]. The results of this study are expected to contribute to the development of efficient and environmentally friendly battery active materials. Thus, the synthesis of  $\text{MnO}_2$  through electrochemical methods can be a strategic solution for future energy.

This study offers novelty by developing a synthesis method for  $\text{MnO}_2$  using electrochemical techniques that have not been widely applied in the context of catalyst development for metal-air batteries. Focusing on the effects of parameters such as the number of electrodes, voltage, and acid-base conditions on the characteristics of  $\text{MnO}_2$  provides new insights that can enhance the efficiency and performance of electrocatalysts [29], [30]. The urgency of this study lies in the urgent need to improve the efficiency of metal-air batteries as an environmentally friendly and sustainable energy technology, especially considering the increasing demand for renewable energy and the lack of efficient alternatives for long-term energy storage. By bridging the gap between innovative synthesis methods and practical performance, this study significantly contributes to the development of more reliable and sustainable energy solutions. This study investigates the effect of electrode quantity and voltage on  $\text{MnO}_2$  nanoparticle yield and characteristics under acidic and basic conditions, while also evaluating  $\text{MnO}_2$ 's potential as an electrocatalyst in metal-air batteries.

## 2. RESEARCH METHOD

### 2.1. Research Materials

No.	Material
1.	KMnO <sub>4</sub> 99.5%
2.	H <sub>2</sub> SO <sub>4</sub> 97%
3.	Electrode (Carbon)
4.	Nickel Foam
5.	N-Methylpyrrolidone (NPM)
6.	pVdF
7.	Demin water
8.	KOH 0.6M

### 2.2. Research Equipment Scheme

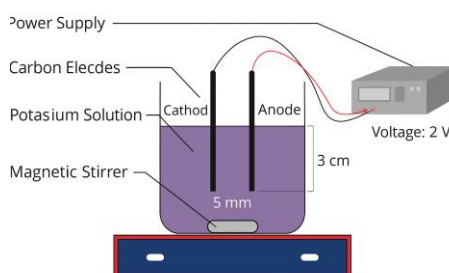


Figure 1. Synthesis of MnO<sub>2</sub> Electrochemical Method with 1 Pair of Electrodes

MnO<sub>2</sub> synthesis was carried out in an electrochemical cell [31], [32]. An electrochemical cell is a 600 ml beaker glass containing an electrolyte solution. In this study, 1 & 4 pairs of electrodes consisting of a cathode and anode were used. Each electrode is connected to a DC power supply whose value will be varied according to the experimental variables used. The anode is connected to the positive pole and the cathode is connected to the negative pole [33], [34]. The following is a multi-electrode MnO<sub>2</sub> synthesis scheme attached in Figure 2:

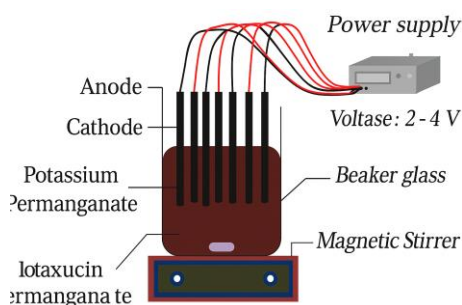


Figure 2. Schematic of MnO<sub>2</sub> Synthesis with 4 Pairs of Electrodes

### 2.3. Research Procedures

#### 2.3.1. Synthesis of MnO<sub>2</sub> in Acidic and Basic Conditions

The MnO<sub>2</sub> synthesis process was carried out in two solution conditions, namely acidic and basic conditions. In acidic conditions, KMnO<sub>4</sub> solution was prepared by dissolving 5 grams of KMnO<sub>4</sub> into 300 mL of demineralized water, then stirred using a magnetic stirrer until homogeneous. Furthermore, 100 mL of H<sub>2</sub>SO<sub>4</sub> solution was added to the solution to produce a solution with an initial pH of around  $\pm 0.2$  before the electrolysis process. The electrolysis process was then carried out for 30 minutes with a voltage of 2 V and 4 V using a DC meter, accompanied by stirring. While in basic conditions, 0.079 M KMnO<sub>4</sub> solution was prepared by mixing 5 grams of KMnO<sub>4</sub> into 400 mL of demineralized water, then 0.1 M KOH was added until the solution pH reached 9. The electrolysis process in basic conditions lasted for 24 hours with the same voltage, namely 2 V and 4 V, using a DC meter and accompanied by stirring. After the electrolysis process, the formed particles are separated from impurities using a sedimentation technique with the help of a centrifuge. The particle sediment is then washed repeatedly with demineralized water until it is clean from contaminants or chemical residues. The separated particles are then dried in a furnace to obtain pure MnO<sub>2</sub> which is ready to be used in the next stage.

### 2.3.2. Preparation of Electrocatalyst Samples

The process of making electrocatalyst samples begins with the preparation of  $\text{MnO}_2$  ink.  $\text{MnO}_2$  powder is mixed evenly with Polyvinylidenedifluoride (pVdF) and N-Methylpyrrolidone (NMP) solvent with a weight ratio of  $\text{MnO}_2$  to pVdF of 10:1. This mixture is stirred until it forms a homogeneous ink. The  $\text{MnO}_2$  ink that has been formed is then printed evenly on the Ni-foam substrate and then dried in a furnace. The dried sample is then used for electrochemical testing, namely the Cyclic Voltammetry (CV) test to observe the  $\text{O}_2$  reduction reaction, and the Linear Polarization test to evaluate the electrocatalytic kinetics rate using the Autolab PGSTAT 302N tool.

### 2.3.3. Electrocatalyst Testing Stage

The electrocatalyst testing stage was carried out after the synthesis and sample printing processes were completed. Electrocatalyst characterization was carried out using the AUTOLAB PGSTAT 302N tool. In the three-electrode electrochemical cell system, the electrocatalyst sample was used as the working electrode, the platinum electrode (Pt) as the counter electrode, and the Ag/AgCl electrode was used as the reference electrode. The electrolyte used in the test was 0.6 M KOH solution. Cyclic voltammetry testing was carried out in 10 cycles at a voltage range from -1 V to +1 V at room temperature, with a scan rate variation of 0.1 V/s. For linear polarization testing, the voltage range used was from -0.1 V to +0.1 V with a scan rate of 0.001 V/s. The visual schematic of the electrocatalyst test system can be seen in Figure 3.

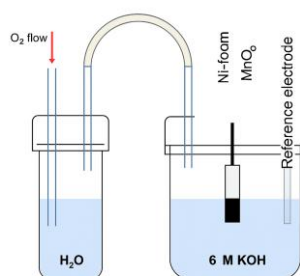


Figure 3. Electrocatalyst Test Scheme

## 2.4. Non-particle $\text{MnO}_2$ Characterization Test

Product characterization was carried out to determine the physical properties and structure of the synthesized  $\text{MnO}_2$  material. The characterization stage began with BET (Brunauer–Emmett–Teller) analysis using the NOVA 1200 Quantachrome series. In this analysis, a small sample was taken from the synthesized product to measure the specific surface area, pore volume, and pore diameter. These parameters are important for determining the potential application of  $\text{MnO}_2$  as an electrocatalyst material, especially in systems with high active surface areas.

Furthermore, characterization was carried out using the XRD (X-Ray Diffraction) technique to identify the crystal structure of the  $\text{MnO}_2$  particles. Through X-ray diffraction, a diffraction pattern (peak) was obtained that reflects the level of purity and type of crystal phase of the synthesized compound. This data is also used to calculate the quantitative percentage of  $\text{MnO}_2$  in the sample. The instrument used for this analysis was the PANalytical series, which has high accuracy in identifying crystalline structures.

In addition, surface morphology characterization was carried out using the SEM (Scanning Electron Microscopy) technique. This technique allows detailed observation of the shape, size, and distribution of  $\text{MnO}_2$  particles down to the nanometer scale. By using high-energy electron beam scattering, SEM provides a visual image of the surface and texture of the synthesized particles. For this purpose, a Zeiss Evo MA 10 tool is used which is capable of producing high-resolution images to support comprehensive material morphology analysis.

## 3. RESULTS AND DISCUSSION

### 3.1. The Effect of Variations in the Number of Electrodes, Voltage and $\text{KMnO}_4$ Concentration on the Yield Produced

From the stage of the  $\text{MnO}_2$  synthesis process using the electrolysis method, variations in the number of electrodes and voltages were used for both conditions, acidic and basic. Because, from this process it is desired to obtain a higher  $\text{MnO}_2$  yield compared to previous studies. With an initial  $\text{KMnO}_4$  mass of 5 grams, a mass yield of 31.38% was produced for acid and 2.34% in basic conditions. By using a new scheme in the electrolysis process,  $\text{MnO}_2$  was produced with a higher product. The following are the results of the  $\text{MnO}_2$  synthesis in variations in the number of electrodes and voltages, with an initial mass of reactants of 5 grams and an initial mole of reactants ( $\text{KMnO}_4$ ) of 0.032 moles which can be summarized in the following table:

Table 2. Comparison of MnO<sub>2</sub> Synthesis Results

Condition	Number of Electrodes	Voltage (V)	Sediment Mass (gr)	Mol of Precipitate (mol)	Mass Yield (%)	Yield Mol (%)
Acidic	2	2	2.0504	0.0236	1.01	74.54
	8	2	2.9552	0.0340	9.10	107.43
	8	4	4.8024	0.0552	6.05	174.59
Basic	2	2	0.1058	0.0012	2.12	2.85
	8	2	0.2926	0.0034	5.85	10.64
	8	4	0.5570	0.0064	1.14	20.25

From the table above, it can be seen that MnO<sub>2</sub> synthesized in acidic conditions has a higher yield than MnO<sub>2</sub> synthesized in basic conditions. The results of the synthesis between acidic and basic conditions show quite different results in the variation of variables used, both for the solution conditions, the number of electrodes and the voltage. For example, MnO<sub>2</sub> synthesized in acidic conditions with 2 electrodes and 2 volts electrolysis has a mass yield of 41.01% while in basic conditions with the addition of 0.1 M KOH solution until the pH reaches 9 only produces a yield of 2.12%. The addition of H<sub>2</sub>SO<sub>4</sub> is an important factor that influences this difference in yield because in acidic conditions it supports the acceleration of the nucleation rate and growth of MnO<sub>2</sub> particles so that the particles formed will be more numerous and tend to be large [35], [36].

This can be explained because in an acidic atmosphere, the MnO<sub>4</sub><sup>-</sup> ion will react with the H<sup>+</sup> ion from H<sub>2</sub>SO<sub>4</sub>, this ion causes the amount of yield produced to be greater. In an acidic atmosphere, the current conducted during the electrolysis process is higher than in a base, based on Faraday's Law, the amount of equivalent electricity flowed is proportional to the amount of substance produced. While in a basic atmosphere, many MnO<sub>4</sub><sup>-</sup> ions have not been decomposed so that a longer electrolysis time is also needed, namely 24 hours when compared to an acidic atmosphere which only takes 30 minutes. Another variable used to produce a maximum MnO<sub>2</sub> yield is the number of electrodes, namely 2 and 8 carbon electrodes. If the number of electrodes is varied, the results obtained are that MnO<sub>2</sub> synthesized using 2 electrodes has a smaller yield than MnO<sub>2</sub> synthesized using 8 electrodes or the number of electrodes is directly proportional to the yield produced in acidic and basic conditions. This is because the use of multi-electrodes causes the surface area of the electrodes used to become larger, thus providing a larger surface as a place for chemical reactions to form MnO<sub>2</sub> nanoparticles. However, when compared between the yields produced between MnO<sub>2</sub> synthesized with 2 and 8 electrodes, the product increase was not significant up to 4 times, this is because the same voltage was used in the electrolysis process, so the current produced was also the same.

Then, the voltage value also affects the MnO<sub>2</sub> produced. The amount of voltage is directly proportional to the yield of MnO<sub>2</sub> produced. The greater the voltage applied during the electrolysis process, the more MnO<sub>4</sub><sup>-</sup> is reduced and forms MnO<sub>2</sub>. However, from the research we did for the synthesis of MnO<sub>2</sub>, it was only used up to a voltage limit of 4 V. Because, when this voltage is used, corrosion begins to occur on the carbon electrode used, so it must be separated from the solution during the washing process with a centrifuge.

Another factor that influences is the concentration of KMnO<sub>4</sub> used for the electrolysis process. In this case, only different concentrations were used for acidic and basic conditions during the electrolysis process, namely 0.0632 M; 0.079 M and 0.105 M. The yield results obtained are as follows:

Table 3. Comparison of MnO<sub>2</sub> Synthesis 2 Electrodes

Condition	Concentration (M)	Amount of Sediment (gr)	Mol of Precipitate (mol)	Mass Yield (%)	Yield Mol (%)
Acidic	0.079	2.0504	0.0236	41.01	74.54
	0.0632	2.9298	0.0337	58.60	106.51
Basic	0.105	0.0760	0.0009	1.52	2.76
	0.079	0.1058	0.0012	2.12	3.85

In these different concentrations, the same mass of KMnO<sub>4</sub> was used, namely 5 grams for both. However, what makes the difference is the amount of demin water dissolved. In an acidic atmosphere, for a concentration of 0.0632 M, 400 ml of demin water + 100 ml of H<sub>2</sub>SO<sub>4</sub> were added. For a concentration of 0.079 M, 300 ml of demin water + 100 ml of H<sub>2</sub>SO<sub>4</sub> were added. Meanwhile, in a basic atmosphere, there were two types of concentrations tested, namely 0.105 M and 0.079 M. With the addition of 300 ml (0.105 M) and 400 ml (0.079 M) of demin water.

From the results that have been displayed, it can be seen that the more concentrated the concentration used for electrolysis, the lower the yield obtained. This is because the more dilute the solution used, the lower the resistance and the greater the activity, so that the MnO<sub>4</sub><sup>-</sup> ions that are reduced to MnO<sub>2</sub> will also be greater. And vice versa.

When viewed from the overall yield mole data produced in each synthesis condition, there is a synthesis condition in acidic conditions that has a yield above 100%, namely for synthesis conditions with 8 electrodes 2 and 4V. This is because there is still a possibility that there are impurities other than MnO<sub>2</sub> in the precipitate, one of which is carbon which acts as an electrode. Indicated by the reduction in carbon mass between before and after the electrolysis process, so that there is carbon that is corroded and mixed in the precipitate.

### 3.2. The Effect of MnO<sub>2</sub> Synthesis Atmosphere on its Performance as an Electrocatalyst in Metal Air Batteries

As previously explained, there are two types of reactions involved in metal air batteries, namely Oxygen Reduction Reaction (ORR) and Oxygen Evolution Reaction (OER). To find out the two reactions, a linear polarization test is carried out. In the linear polarization graph, the ORR area is in the cathodic area. Namely on the left side of the zero potential value ( $V = 0$ ), or which has a negative value. Meanwhile, the OER area is on the right side of the zero potential ( $V = 0$ ), or which has a positive value. Polarization itself occurs when the potential on the electrode surface shifts towards its equilibrium value, resulting in an electrochemical reaction. Some chemical reactions are not single reactions, especially reactions involving more than one electron. Each single reaction has its own kinetic rate.

The series of tools used for linear polarization testing are the same as those used for Cyclic Voltammetry (CV) testing, namely working electrode (Ni-Foam with MnO<sub>2</sub> loading), counter electrode (platinum), reference electrode (Ag/AgCl), and the electrolyte used is KOH 0.6 M. From the test results, a graph plot was made between current density and voltage, and Open Circuit Potential (OCP) data was also obtained. OCP is the zero current potential or resting potential at each electrode. When  $i_o = 0$ , there is a voltage provided by an external power supply. To determine the electrocatalyst performance that can be produced in each variable, it can be reviewed from the highest current density that can be produced in each sample for MnO<sub>2</sub> 2 and 8 Electrodes. The following are the results of the highest current that can be produced in every 1 cm<sup>2</sup> of MnO<sub>2</sub> used:

Table 4. Current Density Comparison

Variable	Number of Electrodes	Voltage	OCP	Current Density (mA.cm <sup>-2</sup> )
Acidic 0.063 M	2	2	0.097	0.128
	2	2	-0.001	0.136
	8	2	-0.156	0.172
Acidic 0.079 M	8	4	-0.115	0.127
	2	2	-0.206	0.023
	2	2	-0.056	0.016
Basic 0.105 M	8	2	-0.013	0.017
	8	4	-0.057	0.012

From the data obtained, it can be concluded that MnO<sub>2</sub> synthesized in acidic conditions tends to have a high current density as a metal air battery. This is because in acidic conditions it tends to form a crystalline structure with  $\beta$ -,  $\alpha$ -,  $\gamma$ - or  $\delta$ -MnO<sub>2</sub> polymorphisms. The electrocatalytic ability of MnO<sub>2</sub> with different polymorphic structures has an increasing ability from  $\beta$ - <  $\lambda$ - <  $\gamma$ - <  $\alpha$ -. The reason is, the crystalline structure tends to have a tunnel with a larger size than amorphous, with  $\alpha$ -MnO<sub>2</sub> with the largest tunnel size, namely (2x2) and (1x1). Thus,  $\alpha$  MnO<sub>2</sub> is a crystallinity structure that has the potential to produce the highest current density compared to other structures. Conversely, amorphous crystallinity will cause its particles to be composed of various tunnels that create high barriers and make it difficult for the diffusion of cations and anions [24], [37].

On the other hand, the results of linear polarization analysis showed that MnO<sub>2</sub> is less effective in its performance as an OER catalyst. Therefore, further research is needed to improve its use as an OER catalyst. One way that can be done is by mixing MnO<sub>2</sub> with other materials derived from carbon or other conductive polymers. Meanwhile, to produce a catalyst that has both ORR and OER capabilities, it is obtained from the synthesis of metal oxides such as Mn<sub>3</sub>O<sub>4</sub> using electrodeposition and calcination methods at a temperature of 480oC [38]-[40].

This research has the potential to make a significant impact in improving the efficiency of metal-air batteries through the development of a more targeted MnO<sub>2</sub> synthesis method, which can produce high-performance electrocatalysts for sustainable energy applications. In addition, the results of this study can open up new opportunities to optimize the design of electrochemical materials by utilizing process parameters such as the number of electrodes and voltage. However, this study has several limitations, such as the limitations in the laboratory scale that may be different from industrial applications, and the need for more in-depth analysis of the long-term stability of the catalyst under complex operational conditions. Further testing in various environmental conditions and collaboration with the industrial sector are needed to ensure that the results of this study can be implemented widely.

#### 4. CONCLUSION

Based on the research that has been done, it can be concluded that the yield of MnO<sub>2</sub> particles produced is proportional to the number of electrodes and the voltage used. The more the number of electrodes and the higher the voltage applied, the higher the yield produced. The yield in this study also showed a significant increase compared to the results of previous studies. This indicates that operational parameters greatly affect the efficiency of MnO<sub>2</sub> synthesis. In addition, the nature of the MnO<sub>2</sub> particles formed is influenced by the pH conditions of the solution. In acidic conditions, particles tend to form crystals resembling  $\alpha$ -MnO<sub>2</sub> with a larger particle diameter but a smaller surface area. Conversely, in basic conditions, the crystals formed resemble  $\gamma$ -MnO<sub>2</sub> with a smaller particle diameter but a larger surface area. This variation indicates that the pH of the solution plays an important role in controlling the morphology and physical properties of the MnO<sub>2</sub> particles produced.

The electrocatalytic test results showed that MnO<sub>2</sub> particles have the ability to reduce oxygen, as evidenced by the emergence of a cathode peak potential with an E<sup>0</sup> value equivalent to the O<sub>2</sub> reduction reaction. Interestingly, MnO<sub>2</sub> synthesized in acidic conditions showed better electrocatalytic performance compared to that synthesized in basic conditions. The highest current density was recorded at 0.172 mA cm<sup>-2</sup>, which was obtained under acidic MnO<sub>2</sub> synthesis conditions using 8 electrodes and a voltage of 2V. Further research can explore the effect of electrolyte and temperature variations during the electrochemical process on the structure and performance of MnO<sub>2</sub> as an electrocatalyst. In addition, long-term testing on metal-air battery prototypes under real operational conditions is needed to ensure the stability and efficiency of this catalyst.

#### ACKNOWLEDGEMENTS

We would like to thank all parties who have supported this research.

#### REFERENCES

- [1] L. Li, Z. Chang, and X. Zhang, "Recent Progress on the Development of Metal-Air Batteries," *Adv. Sustain. Syst.*, vol. 1, no. 10, pp. 1–10, Oct. 2017, doi: 10.1002/adsu.201700036.
- [2] Q. Sun, L. Dai, T. Luo, L. Wang, F. Liang, and S. Liu, "Recent advances in solid-state metal–air batteries," *Carbon Energy*, vol. 5, no. 2, pp. 1–10, Feb. 2023, doi: 10.1002/cey2.276.
- [3] X. Yu and A. Manthiram, "Sustainable Battery Materials for Next-Generation Electrical Energy Storage," *Adv. Energy Sustain. Res.*, vol. 2, no. 5, pp. 1–10, May 2021, doi: 10.1002/aesr.202000102.
- [4] D. Ahuja, V. Kalpna, and P. K. Varshney, "Metal air battery: A sustainable and low cost material for energy storage," *J. Phys. Conf. Ser.*, vol. 1913, no. 1, pp. 1–12, 2021, doi: 10.1088/1742-6596/1913/1/012065.
- [5] P. Stabile, F. Ballo, G. Mastinu, and M. Gobbi, "An ultra-efficient lightweight electric vehicle—power demand analysis to enable lightweight construction," *Energies*, vol. 14, no. 3, pp. 1–18, 2021, doi: 10.3390/en14030766.
- [6] D. Golovanov *et al.*, "4-MW Class High-Power-Density Generator for Future Hybrid-Electric Aircraft," *IEEE Trans. Transp. Electrification*, vol. 7, no. 4, pp. 2952–2964, 2021, doi: 10.1109/TTE.2021.3068928.
- [7] H. Cheng, T. Wang, Z. Li, C. Guo, J. Lai, and Z. Tian, "Anode Interfacial Layer Construction via Hybrid Inhibitors for High-Performance Al–Air Batteries," *ACS Appl. Mater. Interfaces*, vol. 13, no. 43, pp. 51726–51735, Nov. 2021, doi: 10.1021/acsami.1c14829.
- [8] Q. Li, L. Han, Q. Luo, X. Liu, and J. Yi, "Towards Understanding the Corrosion Behavior of Zinc-Metal Anode in Aqueous Systems: From Fundamentals to Strategies," *Batter. Supercaps*, vol. 5, no. 4, pp. 1–10, Apr. 2022, doi: 10.1002/batt.202100417.
- [9] Q. Li *et al.*, "Improving the oxygen redox reversibility of Li-rich battery cathode materials via Coulombic repulsive interactions strategy," *Nat. Commun.*, vol. 13, no. 1, pp. 1–13, 2022, doi: 10.1038/s41467-022-28793-9.
- [10] G. Xu, L. Yang, J. Li, C. Liu, W. Xing, and J. Zhu, "Strategies for improving stability of Pt-based catalysts for oxygen reduction reaction," *Adv. Sens. Energy Mater.*, vol. 2, no. 2, pp. 1–14, 2023, doi: 10.1016/j.asems.2023.100058.
- [11] J. Liu *et al.*, "Rationally Designing Efficient Electrocatalysts for Direct Seawater Splitting: Challenges, Achievements, and Promises," *Angew. Chemie*, vol. 134, no. 45, p. e202210753, Nov. 2022, doi: 10.1002/ange.202210753.
- [12] F. Guo, T. J. Macdonald, A. J. Sobrido, L. Liu, J. Feng, and G. He, "Recent Advances in Ultralow-Pt-Loading Electrocatalysts for the Efficient Hydrogen Evolution," *Adv. Sci.*, vol. 10, no. 21, pp. 1–23, Jul. 2023, doi: 10.1002/advs.202301098.
- [13] C. Das, N. Sinha, and P. Roy, "Transition Metal Non-Oxides as Electrocatalysts: Advantages and Challenges," *Small*, vol. 18, no. 28, p. 2202033, Jul. 2022, doi: 10.1002/sml.202202033.
- [14] W. Xiong, H. Yin, T. Wu, and H. Li, "Challenges and Opportunities of Transition Metal Oxides as Electrocatalysts," *Chem. – A Eur. J.*, vol. 29, no. 5, p. e202202872, Jan. 2023, doi: 10.1002/chem.202202872.
- [15] Y. Yao, L. Zhang, Y. Qiu, Z. Li, Z. Ma, and S. Wang, "Phase–activity relationship of MnO<sub>2</sub> nanomaterials in periodate oxidation for organic pollutant degradation," *Water Res.*, vol. 264, p. 122224, Oct. 2024, doi: 10.1016/j.watres.2024.122224.
- [16] A. K. Worku, D. W. Ayele, N. G. Habtu, M. A. Teshager, and Z. G. Workineh, "Recent progress in MnO<sub>2</sub>-based oxygen electrocatalysts for rechargeable zinc-air batteries," *Mater. Today Sustain.*, vol. 13, p. 100072, Sep. 2021, doi: 10.1016/j.mtsust.2021.100072.
- [17] F. Bibi, A. Numan, Y. S. Tan, and M. Khalid, "Facile extraction of Mo<sub>2</sub>Ti<sub>2</sub>C<sub>3</sub>T<sub>x</sub> MXene via hydrothermal synthesis for electrochemical energy storage," *J. Energy Storage*, vol. 85, p. 111154, Apr. 2024, doi: 10.1016/j.est.2024.111154.
- [18] K. Hachem *et al.*, "Methods of Chemical Synthesis in the Synthesis of Nanomaterial and Nanoparticles by the Chemical

- Deposition Method: A Review,” *Bionanoscience*, vol. 12, no. 3, pp. 1032–1057, 2022, doi: 10.1007/s12668-022-00996-w.
- [19] H. Li *et al.*, “Revisiting the Preparation Progress of Nano-Structured Si Anodes toward Industrial Application from the Perspective of Cost and Scalability,” *Adv. Energy Mater.*, vol. 12, no. 7, p. 2102181, Feb. 2022, doi: 10.1002/aenm.202102181.
- [20] V. Harish *et al.*, “Cutting-edge advances in tailoring size, shape, and functionality of nanoparticles and nanostructures: A review,” *J. Taiwan Inst. Chem. Eng.*, vol. 149, no. March, p. 105010, 2023, doi: 10.1016/j.jtice.2023.105010.
- [21] J. Łuczak, M. Kroczevska, M. Baluk, J. Sowik, P. Mazierski, and A. Zaleska-Medynska, “Morphology control through the synthesis of metal-organic frameworks,” *Adv. Colloid Interface Sci.*, vol. 314, no. February, pp. 1–31, 2023, doi: 10.1016/j.cis.2023.102864.
- [22] M.-R. Zamani-Meymian, K. Khanmohammadi Chenab, and H. Pourzolfaghar, “Designing High-Quality Electrocatalysts Based on CoO:MnO<sub>2</sub>@C Supported on Carbon Cloth Fibers as Bifunctional Air Cathodes for Application in Rechargeable Zn–Air Battery,” *ACS Appl. Mater. Interfaces*, vol. 14, no. 50, pp. 55594–55607, Dec. 2022, doi: 10.1021/acsami.2c16826.
- [23] Y. Li *et al.*, “Ultra-Low Pt Doping and Pt–Ni Pair Sites in Amorphous/Crystalline Interfacial Electrocatalyst Enable Efficient Alkaline Hydrogen Evolution,” *Small*, vol. 19, no. 23, p. 2300368, Jun. 2023, doi: 10.1002/sml.202300368.
- [24] J. Zhang, Y. Li, Z. Chen, Q. Liu, Q. Chen, and M. Chen, “Amorphous Electrode: From Synthesis to Electrochemical Energy Storage,” *ENERGY Environ. Mater.*, vol. 6, no. 6, p. e12573, Nov. 2023, doi: 10.1002/eem2.12573.
- [25] Y. Zhang, D. Wang, C. Ye, F. Gao, Z. Li, and Y. Du, “Regulation of crystallinity and defects on CoNiRuOx nanocages for enhanced oxygen evolution reaction,” *Chem. Eng. J.*, vol. 466, p. 143059, Jun. 2023, doi: 10.1016/j.cej.2023.143059.
- [26] Y. Chen *et al.*, “Molecular Engineering toward High-Crystallinity Yet High-Surface-Area Porous Carbon Nanosheets for Enhanced Electrocatalytic Oxygen Reduction,” *Adv. Sci.*, vol. 9, no. 3, p. 2103477, Jan. 2022, doi: 10.1002/advs.202103477.
- [27] X. Yi, Y. Song, D. He, W. Li, A. Pan, and C. Han, “Constructing a high-performance bifunctional MnO<sub>2</sub>-based electrocatalyst towards applications in rechargeable zinc–air batteries,” *J. Mater. Chem. A*, vol. 12, no. 43, pp. 29355–29382, 2024, doi: 10.1039/D4TA05182C.
- [28] M. Karimpour, M. Dorri, A. Babaei, C. Zamani, M. Soleimani, and M. Pourfath, “New insights on the effects of surface facets and calcination temperature on electrochemical properties of MnCo<sub>2</sub>O<sub>4</sub> as bifunctional oxygen electrocatalyst in zinc-air batteries,” *Electrochim. Acta*, vol. 467, p. 143022, Nov. 2023, doi: 10.1016/j.electacta.2023.143022.
- [29] Y.-Y. Lee *et al.*, “Recent Advances in Electrocatalytic Transesterification: Enhancing Biodiesel Synthesis for Sustainable Energy,” *Int. J. Energy Res.*, vol. 2025, no. 1, p. 7887020, Jan. 2025, doi: 10.1155/er/7887020.
- [30] R. Kulkarni *et al.*, “Exploring the recent cutting-edge applications of CNTs in energy and environmental remediation: Mechanistic insights and remarkable performance advancements,” *J. Environ. Chem. Eng.*, vol. 12, no. 5, p. 113251, Oct. 2024, doi: 10.1016/j.jece.2024.113251.
- [31] L. Zeng, G. Zhang, X. Huang, H. Wang, T. Zhou, and H. Xie, “Tuning crystal structure of MnO<sub>2</sub> during different hydrothermal synthesis temperature and its electrochemical performance as cathode material for zinc ion battery,” *Vacuum*, vol. 192, p. 110398, Oct. 2021, doi: 10.1016/j.vacuum.2021.110398.
- [32] A. Tounsi *et al.*, “One-step electrochemical synthesis of FTO/MnO<sub>2</sub>-graphene composite for electrochemical energy storage,” *J. Energy Storage*, vol. 73, p. 109228, Dec. 2023, doi: 10.1016/j.est.2023.109228.
- [33] Z. Lin, S. Cheng, Z. Yu, J. Yang, H. Huang, and Y. Sun, “Enhancing bio-cathodic nitrate removal through anode-cathode polarity inversion together with regulating the anode electroactivity,” *Sci. Total Environ.*, vol. 764, p. 142809, Apr. 2021, doi: 10.1016/j.scitotenv.2020.142809.
- [34] A. A. Samkov *et al.*, “Decolorization of Dyes in a Bioelectrochemical System Depending on the Immobilization of *Shewanella oneidensis* Mr-1 Cells on the Anode Surface and Electrical Stimulation of an External Circuit,” *Appl. Biochem. Microbiol.*, vol. 59, no. 2, pp. 198–205, Apr. 2023, doi: 10.1134/S0003683823020096.
- [35] K.-J. Wu, E. C. M. Tse, C. Shang, and Z. Guo, “Nucleation and growth in solution synthesis of nanostructures – From fundamentals to advanced applications,” *Prog. Mater. Sci.*, vol. 123, p. 100821, Jan. 2022, doi: 10.1016/j.pmatsci.2021.100821.
- [36] P. Sharma, P. Parashar, D. Ghosh, D. Yadav, P. Rawat, and S. Majumder, “A Review on Microwave Assisted Synthesis of Transition Metal Oxides and their Potent Application as Supercapacitors,” *ChemistrySelect*, vol. 8, no. 47, p. e202303467, Dec. 2023, doi: 10.1002/slct.202303467.
- [37] Z. Liu *et al.*, “Ion migration and defect effect of electrode materials in multivalent-ion batteries,” *Prog. Mater. Sci.*, vol. 125, p. 100911, Apr. 2022, doi: 10.1016/j.pmatsci.2021.100911.
- [38] Y.-D. Dong *et al.*, “Synthesis of Fe–Mn-Based Materials and Their Applications in Advanced Oxidation Processes for Wastewater Decontamination: A Review,” *Ind. Eng. Chem. Res.*, vol. 62, no. 28, pp. 10828–10848, Jul. 2023, doi: 10.1021/acs.iecr.3c01624.
- [39] L. Hao, J. H. Yang, G. Li, P. Li, and Y. Cao, “Development and challenges of coal-based graphene family nanomaterials,” *Rev. Inorg. Chem.*, pp. 1–25, 2025, doi: 10.1515/revic-2024-0101.
- [40] A. M. Butt, M. Batool, M. A. Jaoude, and A. Qurashi, “Recent advancement in manganese-based electrocatalyst for green hydrogen production,” *J. Electroanal. Chem.*, vol. 937, p. 117393, May 2023, doi: 10.1016/j.jelechem.2023.117393.